# Direct Observation of Irrotational Flow and Evidence of Superfluidity in a Rotating Bose-Einstein Condensate

G. Hechenblaikner, E. Hodby, S. A. Hopkins, O. M. Maragò,* and C. J. Foot

*Clarendon Laboratory, Department of Physics, University of Oxford, Parks Road, Oxford OX1 3PU, United Kingdom*

(Received 9 June 2001; published 31 January 2002)

We have observed the expansion of vortex-free, rotating Bose condensates after their sudden release from a slowly rotating anisotropic trap. Conservation of angular momentum, combined with the constraint of irrotational flow, cause the rotating condensate to expand in a distinctively different way to one released from a static (nonrotating) trap. This difference provides clear experimental evidence of the purely irrotational velocity field associated with a superfluid. We observed this behavior in absorption images taken along the rotation axis.

DOI: 10.1103/PhysRevLett.88.070406 PACS numbers: 03.75.Fi, 05.30.Jp, 32.80.Pj, 67.90.+z

The term superfluidity was originally coined to describe the striking experimental properties of liquid helium-4, such as nonviscous flow, persistent currents, and quantized vortices. Superfluid behavior has also been observed in Fermi-degenerate quantum liquids such as helium-3 and nuclear matter (nuclei and neutron stars). Since the creation of the first alkali metal Bose condensates [1], there has been great interest in observing the superfluid properties of these systems, such as the absence of viscous dissipation below a critical velocity [2] and the production of quantized vortices [3–5] when the condensate rotates with a sufficiently high angular velocity. Vortex creation is a direct consequence of the fundamental constraint on superfluids that they have irrotational flow [6]. However, this property of purely irrotational flow may also be observed in the case of rotating, vortex-free condensates. One recent experiment used the frequency of the scissors mode oscillation to show that the condensate has a quenched moment of inertia [7,8]. (The scissors mode is a small angle oscillation of the condensate shape, with zero mean angular momentum.) Another case of interest, recently studied theoretically by Edwards *et al.* [9], occurs when a condensate rotating below the critical angular velocity for vortex nucleation is released from the trap and expands. In their paper [9], Edwards *et al.* calculated the time evolution of this expansion. They show that irrotational flow, together with the conservation of angular momentum, result in expansion behavior that is easily distinguished from that of a nonrotating condensate or a thermal atom cloud. We report here the experimental verification of their predictions by time-of-flight measurements on a condensate released from a rotating anisotropic trap [10]. We directly observe the irrotational flow in this vortex-free condensate, thus giving further evidence for the superfluidity of Bose-condensed gases. This work is complementary to the evidence of superfluidity in condensates containing vortices.

The solutions of the hydrodynamic equations for superfluids [11] show that a condensate always has a moment inertia less than that of a rigid body of the same mass distribution [12]. For the special case of axial symmetry, the superfluid has zero moment of inertia about the symmetry axis. Thus a vortex-free condensate with some angular momentum can never be symmetric about the rotation axis, since this would imply the unphysical situation of infinite angular velocity. We observed the effect of this constraint in absorption images of the condensate taken along the direction of the rotational axis—the projection of the cloud in this direction never becomes circular (an aspect ratio of unity). The evolution of the condensate density distribution, calculated using the hydrodynamic equations in [9], agrees well with our data. We give a brief review of the underlying theoretical aspects before describing the experimental procedure and results.

In our experiment we have an anisotropic harmonic potential with three angular frequencies $\omega_x < \omega_y < \omega_z$. The potential rotates about the $z$ axis with angular frequency $\Omega$. It is convenient to define two new parameters: the trap deformation, $\lambda = (\omega_x^2 - \omega_y^2)/(\omega_x^2 + \omega_y^2)$, and the mean square of the frequencies in the plane of rotation, $\omega_m^2 = (\omega_x^2 + \omega_y^2)/2$. In the hydrodynamic limit, a condensate rotating in this trap displays a quadrupolar flow pattern, as described in Fig. 1, and has a wave function which looks like (in the lab frame)

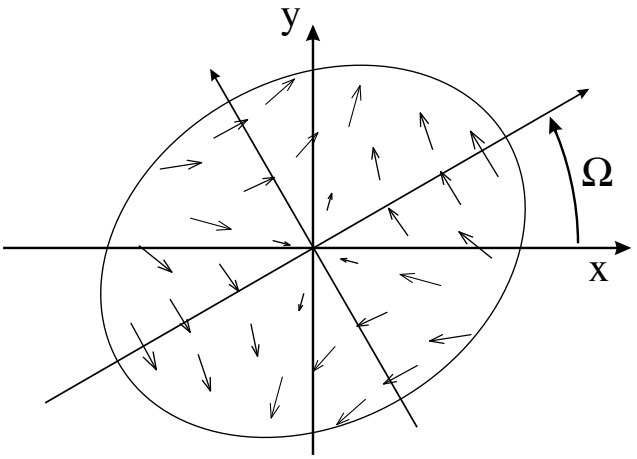


FIG. 1. The velocity field of a vortex-free condensate in an elliptical trap, rotating at frequency $\Omega$. The small arrows of the velocity field indicate the direction of the quadrupolar flow.

  

$$\Psi(\mathbf{r}) = \sqrt{\rho(\mathbf{r})}\, e^{i m \nu x y/\hbar}, \tag{1}$$

where $\rho(\mathbf{r})$ is the condensate density given in Eq. (3) below. The quadrupole frequency, $\nu$, can be found from the solutions of the following cubic equation [13]:

$$\tilde{\nu}^3 + (1 - 2\tilde{\Omega}^2)\tilde{\nu} + \lambda\tilde{\Omega} = 0, \tag{2}$$

where we introduced the dimensionless quantities $\tilde{\nu} = \nu/\omega_m$ and $\tilde{\Omega} = \Omega/\omega_m$.

In a rotating trap, the condensate experiences modified trapping frequencies because of its quadrupolar motion. The condensate density can be written as

$$\rho(\mathbf{r}) = \frac{\mu}{g}\left[1 - \frac{m}{2}(\tilde{\omega}_x^2 x^2 + \tilde{\omega}_y^2 y^2 + \omega_z^2 z^2)\right]. \tag{3}$$

The modified frequencies $\tilde{\omega}_x$ and $\tilde{\omega}_y$ are given by

$$\begin{aligned} \tilde{\omega}_x^2 &= \omega_x^2 + \nu^2 - 2\nu\Omega, \\ \tilde{\omega}_y^2 &= \omega_y^2 + \nu^2 + 2\nu\Omega, \end{aligned} \tag{4}$$

where $\nu$ is found from Eq. (2).

Hence, the aspect ratio of the condensate in the trap is

$$\frac{R_x}{R_y} = \frac{\tilde{\omega}_y}{\tilde{\omega}_x} = \sqrt{\frac{\Omega + \nu}{\Omega - \nu}}, \tag{5}$$

where $R_x, R_y$ are the sizes of the condensate in the $x$ and $y$ directions, respectively. The effective chemical potential and condensate sizes in the trap can also be calculated from Eqs. (4).

To calculate the expansion of a condensate when released from the anisotropic harmonic potential, we use the following ansatz for the condensate density $\rho(\mathbf{r}, t)$ and the velocity field $\mathbf{v}(\mathbf{r}, t)$ in the Thomas-Fermi regime (as in [9]):

$$\begin{aligned} \rho(\mathbf{r}, t) = \rho_0(t) &- \rho_x(t)x^2 - \rho_y(t)y^2 \\ &- \rho_z(t)z^2 - \rho_{xy}(t)xy, \end{aligned} \tag{6}$$

$$\mathbf{v}(\mathbf{r}, t) = \tfrac{1}{2}\nabla[\upsilon_x(t)x^2 + \upsilon_y(t)y^2 + \upsilon_z(t)z^2 + \upsilon_{xy}(t)xy]. \tag{7}$$

Inserting this ansatz into the hydrodynamic equations of superfluids [11] yields a set of nine coupled differential equations for the expansion parameters, which we integrate numerically. The initial conditions for the density are found from Eq. (3). Note that the cross term $\rho_{xy}(0)$ is assumed to be zero at the instant when the condensate is released from the trap. During the evolution in time of flight, this term grows and can become comparable in size to $\rho_x$, so that the elliptical condensate rotates with respect to its initial release angle. All components of the velocity field are initially zero, except for the cross term, which is the quadrupole velocity field of the rotating condensate, given by $\upsilon_{xy} = 2\nu$ [see Eq. (1)]. The behavior of the condensate is thus completely determined by the above initial conditions and the nine coupled differential equations [9].

The angle of the condensate and its sizes can be found by diagonalizing the quadratic form defined in Eq. (6). Initially one finds that the condensate expands most rapidly along its smaller axis so that its shape becomes more circular. However, the condensate has a quadrupolar flow pattern (see Fig. 1) and an associated angular momentum. Conservation of this angular momentum prevents the condensate from becoming completely axially symmetric (i.e., with a circular cross section), as a cylindrical quadrupolar flow pattern has no angular momentum. So after reaching a critical minimum aspect ratio, it expands most rapidly along its original long axis and hence the aspect ratio increases again. Close to the critical aspect ratio the moment of inertia also reaches a minimum value and hence a peak is observed in the angular velocity [9]. Energy conservation limits how fast the condensate can rotate and hence sets the minimum value for the aspect ratio. In contrast, a thermal gas can have an axially symmetric density distribution and preserve angular momentum, since there are no constraints of irrotationality. Thus it is essentially the superfluid nature of the Bose condensate which prevents it from having a circular cross section.

To observe this behavior we evaporatively cooled $^{87}$Rb atoms in a time-averaged orbiting potential (TOP) trap to a temperature of $0.5T_c$, where $T_c$ is the critical temperature for condensation. This produced Bose condensates of $1.5 \times 10^4$ atoms, in a trapping potential with frequencies $\omega_x/2\pi = \omega_y/2\pi = 124$ Hz and $\omega_z/2\pi = 350$ Hz. We then made the trap elliptical with $\omega_y/\omega_x = 1.4$ (corresponding to $\lambda = 0.32$) by changing the ratio of the two TOP-field components to $B_x/B_y = 4.2$. The eccentric trap was rotated by modulating the high frequency sinusoidal TOP signal (7 kHz) at the low trap rotation frequency $\Omega$, as described in [10]. The eccentricity was ramped up from zero to its final value in 500 ms. Then the condensate was left in the rotating trap for another 500 ms before it was released at a fixed reference angle in the trap rotation, from which the angles of the expanding cloud were measured. The left column of Fig. 2 shows typical absorption images of the condensate, taken along the axis of rotation, after different expansion times. For these pictures the trap was rotating at 28 Hz (well below the threshold to nucleate vortices [14]) and at the instant of release the long axis of the cloud was along the $x$ direction. The angle and aspect ratio of the cloud were obtained from a 2D parabolic fit to the density distribution. The cloud reached a minimum aspect ratio of 1.31 after about 4 ms time of flight and the angle approached its asymptotic value of $\sim 55°$ after 16 ms. For comparison, the evolution of a condensate released from a nonrotating trap is shown for the same expansion times in the right column of Fig. 2. In this case the aspect ratio decreased steadily so that the cloud became circular after about 4 ms, and then it continued to expand so that the aspect ratio inverted. Note that the trapping frequencies $\omega_x$ and $\omega_y$ were the same in both columns. The enhanced aspect ratio in the left column, both in the trap and at long

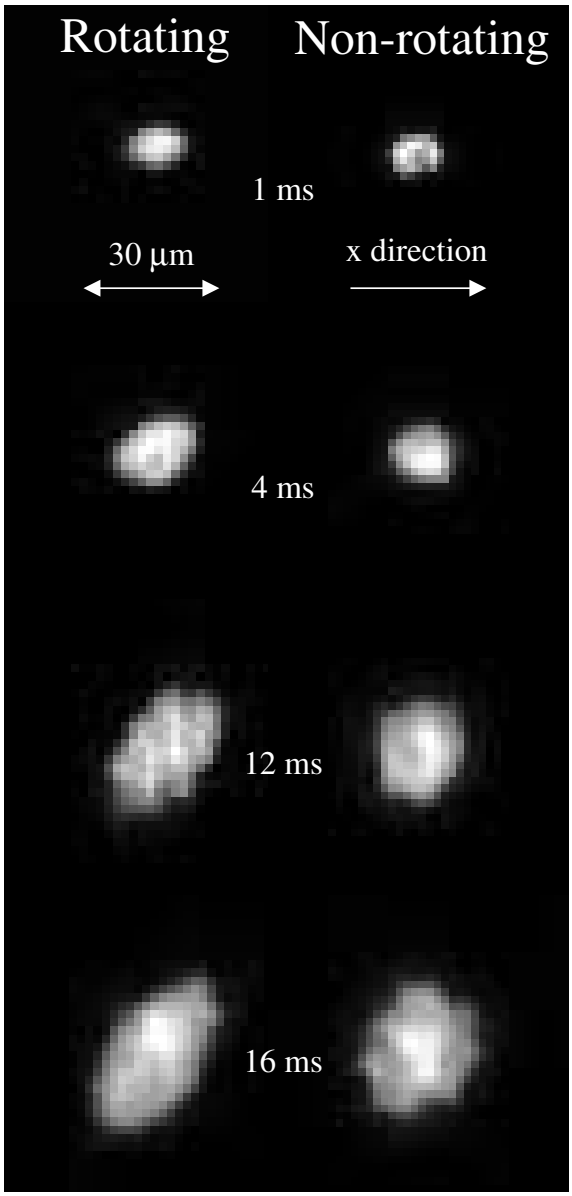


FIG. 2. Typical images of the condensate at different times after release from a trap rotating at 28 Hz (left column) and after release from a nonrotating trap (right column). At the instant of release the long axis of the cloud lay along the $x$ direction. The rotating condensate is observed to have a much larger asymptotic aspect ratio than the static one, as predicted by the upper and lower theoretical curves of Fig. 4.

expansion times, is a result of the irrotational flow pattern in the rotating condensate.

It was necessary to go to a high trap eccentricity to observe the deformation of the cloud clearly. We investigated the evolution of the condensate in time of flight at two different trap rotation frequencies $\Omega/2\pi = 20$ and 28 Hz. In both cases the condensate was released from a trap of $\omega_x/2\pi = 60$ Hz, $\omega_y/2\pi = 1.4 \times 60$ Hz, and $\omega_z/2\pi = 206$ Hz. Figure 3 shows the calculated change of angle of a condensate in time of flight after being released from a trap rotating at $\Omega/2\pi = 20$ Hz (solid line) and $\Omega/2\pi = 28$ Hz (dotted line), with the experimental

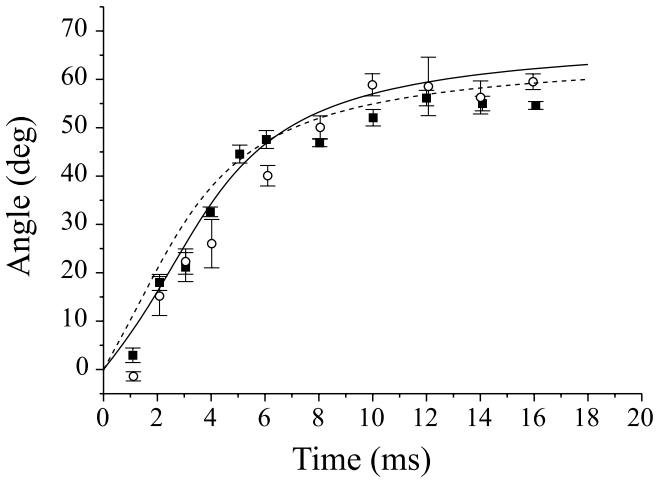


FIG. 3. The angle of the condensate plotted against the time of flight. The open circles and the filled squares denote the measured angles after release from a trap rotating at $\Omega/2\pi = 20$ and 28 Hz, respectively. The solid and the dotted lines are the respective theoretical calculations.

data points superimposed. In both cases the angle evolves in a similar manner; it reaches 45° after about 6 ms. After 18 ms the angle is close to its asymptotic value between 55 and 60°.

Figure 4 shows the theoretical prediction for the evolution of the condensate's aspect ratio in time of flight, with experimentally measured values superimposed, for $\Omega/2\pi = 28$ Hz (upper curve), for $\Omega/2\pi = 20$ Hz (middle curve), and for release from a nonrotating trap (lower curve). The data clearly demonstrate how the aspect ratio for an initially rotating condensate decreases up to a critical point, which is reached after approximately 4 ms. From that point on it does not continue to expand along its minor axis but the aspect ratio increases again because the condensate cannot become circular under these conditions. However, the condensate released from a static trap has no velocity field which prevents it from becoming circular and the aspect ratio decreases steadily from $\omega_y/\omega_x$ (greater than one) to a final value of less than one. Every experimental point displayed is the average of several measurements. For each time of flight we had to refocus our imaging system as the atoms move out of focus under gravity when released from the trap. Incorrect focusing would only result in a more circular image and the minimum value for the measurement of the aspect ratio of rotating condensates was never consistent with unity. There is good agreement between the experimental data and the theoretical predictions at rotation $\Omega/2\pi = 20$ Hz. However, we observed a small deviation of the experimental data from the predicted values for a higher rotation frequency of $\Omega/2\pi = 28$ Hz, shown in the upper curve.

Our results show that an expanding vortex-free Bose condensate with some angular momentum refuses to become circular about the axis of rotation, as predicted by Edwards *et al.* [9]. This provides direct evidence that Bose-condensed gases have purely irrotational flow and

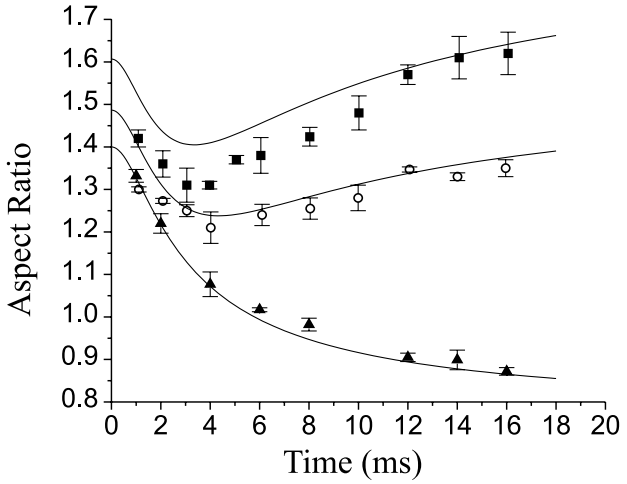


FIG. 4. The aspect ratio of a condensate in time of flight. Initially rotating condensates (upper and middle theoretical curves) exhibit a strong backbending effect after 4 ms and the condensate never becomes circular about the rotation axis. However, after release from the nonrotating trap, the aspect ratio decreases steadily and inverts (lower curve); it is unity at about 6 ms. Upper curve and filled squares: $\Omega/2\pi = 28$ Hz; middle curve and open circles: $\Omega/2\pi = 20$ Hz; lower curve and filled triangles: static trap.

a reduced moment of inertia, as a consequence of their superfluidity. Other measurements of the flow of a Bose-condensed gas would be of great interest, for example, flow through a narrow tube [15] or array of holes, analogous to the superleak experiments with liquid helium.

We thank M. Edwards, S. Stringari, and the members of the Oxford theoretical BEC group for fruitful discussions. We are very grateful to J. Arlt for his contribution to the early stages of this experiment. We acknowledge support from the EPSRC, St. John's College, Oxford (G. H.), Christ Church College, Oxford (E. H.), Linacre College, Oxford, MCFA, and the EC (O. M.).

*Current address: Istituto di Tecniche Spettroscopiche, CNR Via La Farina 237, 98123 MESSINA, Italy.

[1] M. H. Anderson *et al.,* Science **269**, 198 (1995); K. B. Davis *et al.,* Phys. Rev. Lett. **75**, 3969 (1995).

[2] C. Raman, M. Köhl, R. Onofrio, D. S. Durfee, C. E. Kuklewich, Z. Hadzibabic, and W. Ketterle, Phys. Rev. Lett. **83**, 2502 (1999).

[3] M. R. Matthews, B. P. Anderson, P. C. Haljan, D. S. Hall, C. E. Wieman, and E. A. Cornell, Phys. Rev. Lett. **83**, 2498 (1999).

[4] K. W. Madison, F. Chevy, W. Wohlleben, and J. Dalibard, Phys. Rev. Lett. **84**, 806 (2000); K. W. Madison, F. Chevy, V. Bretin, and J. Dalibard, Phys. Rev. Lett. **86**, 4443 (2001).

[5] J. R. Abo-Shaeer, C. Raman, J. M. Vogels, and W. Ketterle, Science **292**, 476 (2001).

[6] P. Nozières and D. Pines, *The Theory of Quantum Liquids* (Perseus Books, Cambridge, MA, 1990).

[7] O. M. Maragò, S. A. Hopkins, J. Arlt, E. Hodby, G. Hechenblaikner, and C. J. Foot, Phys. Rev. Lett. **84**, 2056 (2000).

[8] D. Guéry-Odelin and S. Stringari, Phys. Rev. Lett. **83**, 4452 (1999).

[9] M. Edwards, C. W. Clark, P. Pedri, L. Pitaevskii, and S. Stringari, preceding Letter, Phys. Rev. Lett. **88**, 070405 (2002).

[10] J. Arlt, O. M. Maragò, E. Hodby, S. A. Hopkins, G. Hechenblaikner, S. Webster, and C. J. Foot, J. Phys. B **32**, 5861 (1999).

[11] S. Stringari, Phys. Rev. Lett. **77**, 2360 (1996).

[12] F. Zambelli and S. Stringari, Phys. Rev. A **63**, 033602 (2001).

[13] James Anglin (private communication); Gerald Hechenblaikner, first year report, Clarendon Laboratory, 1999; A. Recati, F. Zambelli, and S. Stringari, Phys. Rev. Lett. **86**, 377 (2001).

[14] E. Hodby, G. Hechenblaikner, S. A. Hopkins, O. M. Maragò, and C. J. Foot, cond-mat/0106262.

[15] B. Jackson, J. F. McCann, and C. S. Adams, J. Phys. B **31**, 4489 (1998).